Available online at www.sciencedirect.com

SCIENCE DIRECT®

Catalysis Today 91–92 (2004) 265–269

CATALYSIS TODAY

www.elsevier.com/locate/cattod

Novel MoVSbO$_x$-type catalysts for selective isobutane oxidation

Johan S. Paul[a], Marijke H. Groothaert[a], Christine E.A. Kirschhock[a], Oleg I. Lebedev[b], Pierre A. Jacobs[a,*], Wilhelm F. Maier[c]

[a] Centrum voor Oppervlaktechemie en Katalyse, KULeuven, Kasteelpark Arenberg 23, B-3001 Heverlee, Belgium
[b] EMAT, Universiteit Antwerpen, Groenenborgerlaan 171, B-2020 Antwerpen, Belgium
[c] Technische Chemie, University of the Saarland, Am Markt, Zeile 3, D-66125 Dudweiler, Germany

Abstract

A new sol–gel synthesis procedure is proposed for the preparation of MoVSbO$_x$ catalysts for the selective oxidation of isobutane. Physico-chemical characterization of the materials calcined at 400 °C, showed essentially amorphous catalysts, with long-range order. Increase of calcination temperature, however, resulted in the formation of small crystalline regions, confirmed through TEM. EPR measurements on the calcined samples pointed to the presence of isolated and magnetically interacting V(IV) species. The reported catalysts proved to be much more selective for partial oxidation compared to a literature reference catalyst. Furthermore, it is shown that this versatile synthesis recipe forms an excellent start for high-throughput and combinatorial studies.

Keywords: Isobutane; Oxidation; Gas-phase; Heterogeneous catalysis; Mo–V–Sb; Mixed oxides; Amorphous; Sol–gel process; Combinatorial chemistry; High-throughput experimentation (hte)

1. Introduction

The direct selective oxidation of isobutane using air is an attractive alternative for the production of methacrolein and methacrylic acid to substitute the acetone cyanohydrine process.

A large variety of catalysts have been studied for the direct oxidation of isobutane to methacrolein and methacrylic acid. The most extensively studied systems are the heteropolyacid (HPA) catalysts [1–8]. Also, several catalytic systems based on mixed oxides have been reported for the partial oxidation of isobutane [9–11]. Driven by the demand for catalysts with increased selectivity and yield, the search for new catalyst formulations and synthesis procedures remains very timely.

In this study a new synthesis procedure was developed to yield highly selective MoVSbO$_x$ oxidation catalysts. These catalysts showed increased selectivity for methacrolein and isobutene, compared to a known literature reference catalyst. Furthermore, this synthesis method allowed easy automation of catalyst preparation by high-throughput techniques. In this way the sol–gel recipe used has already been applied for the optimization of the MoVSbO$_x$ system [12]. On the other hand, the versatility of the recipe allowed to combine many other metal precursors to form several ternary composition diagrams [13].

2. Experimental and methods

For the synthesis of the $Mo_8V_2Sb_{90}O_x$ catalyst, a modified acid-catalyzed sol–gel procedure (Eq. (1)) was applied, based on the synthesis procedure for amorphous mixed oxides [14]:

$$x\,M_1(OR_1)_k + y\,M_2(OR_2)_l + z\,M_3(OR_3)_m + 65\,\text{solvent} + 0.20H^+ \rightarrow \text{mixed oxides} \qquad (1)$$

Metal alkoxide precursor solutions (0.5 M) were prepared by solving commercially available metal alkoxides (vanadium (V) triisopropoxide, molybdenum (V) isopropoxide 5% (w/v) in isopropanol) and an anhydrous metal chloride

---

[*] Corresponding author. Tel.: +32-16321595; fax: +32-16321998.
E-mail address: pierre.jacobs@agr.kuleuven.ac.be (P.A. Jacobs).

0920-5861/$ – see front matter © 2004 Elsevier B.V. All rights reserved.
doi:10.1016/j.cattod.2004.03.041

(antimony (V) chloride) in isopropanol. For metal chlorides in isopropanol, the solutions were flushed with argon in order to remove the formed HCl vapors. The solvent used in all cases was isopropanol, whereas proton acidity originated from a 0.15 M acetic acid solution in isopropanol. After mixing the precursors, the solution was allowed to gelate for 3 days. After drying at 60 °C, the resulting gels were calcined at 250 °C for 5 h at a heating rate of 0.5 °C per minute and at 400 °C for 8 h at a heating rate of 0.5 °C per minute. Alternatively, this catalyst was calcined again at 600 °C in order to examine the influence of the calcination temperature. The reference catalyst ($Mo_{8.3}V_{8.3}Sb_{83.3}O_x$) used was synthesized following the slurry procedure of Shishido et al. [11].

Typically, catalytic tests were carried out at atmospheric pressure in a gas-phase tubular flow quartz reactor between 325 and 450 °C. Catalyst of 2.0 g, pelletized to a 0.125–0.250 mm fraction and diluted with 1.0 g of SiC of the same granule size, was packed between two layers of quartz wool. Using calibrated mass flow controllers, isobutane/oxygen/helium volumetric mixtures in a ratio of 15:5:10 were continuously dosed at a total feed flow of 40 ml min^{-1}. The sol–gel catalysts calcined at 400 °C were activated in situ prior to reaction at 400 °C in a flow of 20% oxygen in helium for 2 h, whereas the ones calcined at 600 °C were activated at 500 °C in a flow of 20% oxygen in helium for 2 h. Feed and products were analyzed with an on-line HP 5890 series II gas chromatograph equipped with: (i) a CP WCOT Fused Silica column connected to a methanizer and an FID, and (ii) a molecular sieve 5 Å column connected to a TCD. This allowed determination of carbon and oxygen mass balances.

The catalysts were characterized using TGA, BET, transmission XRD, TEM and EPR. TGA was performed on a Setaram TG-DTA 92 thermobalance. In a flow of helium containing 20% oxygen, a sample of about 25 mg was heated from room temperature to 800 °C with a heating rate of 5 °C per minute. Nitrogen sorption measurements were recorded with a Coulter Omnisorp 100CX at 77 K. Prior to measurement, the samples (typically 2 g) were outgassed at 100 °C under vacuum overnight. The XRD characterization was carried out at room temperature using a flat sample transmission Rigaku diffractometer. The TEM analyses were performed on a Philips CM20 microscope, operated at an accelerating voltage of 200 kV. X-band EPR spectra were recorded at room temperature and at 120 K with a Bruker ESP 300E instrument in a rectangular TE_{104} cavity. No qualitative difference in the spectral profile was observed by comparing the spectra at these two temperatures. For the simulation of the EPR spectra the Simpow program [15] was used. Quantitative estimation of V(IV) was performed by comparing the spectral intensity at 120 K of each sample (which is the result of a double integration of the experimental first derivative spectrum) with that of frozen aqueous $VOSO_4$ standards of known spin concentration.

3. Results and discussion

3.1. Synthesis and characterization

It has been shown [16] that amorphous microporous silica, titania, zirconia, and alumina with a narrow pore size distribution can be synthesized by a specific sol–gel process in the absence of organic templating agents [14]. These microporous materials form exclusively under acid-catalyzed sol–gel conditions. By adopting this sol–gel process, we have now succeeded in the synthesis of other homogeneous mixed metal oxides (Eq. (1)).

Thermal degradation of the sol–gel prepared catalysts showed a first significant weight loss of about 20% due to the loss of water and isopropanol, which was essentially completed at 200 °C. At temperatures between 300 and 500 °C there was a second significant weight loss of about 12%, attributed to the loss of water from surface hydroxyl groups.

The porosity of the calcined materials was characterized by nitrogen adsorption/desorption isotherms. All mixed oxides calcined at 400 °C showed a substantial adsorption in the P/P_0 region indicating the presence of micropores, whereas a remarkable hysteresis loop indicated the presence of mesopores with a maximum near 40 Å [17]. The specific surface area, calculated with the BET method, amounted to 39 m^2/g. The effective micropore diameters, as determined by the Horvath–Kawazoe method [18], were between 0.6 and 0.7 nm. It seems that the incorporation of organic products during gelation and their release during the slow and careful drying of these materials is responsible for the pore size and porosity of the final products. Calcining the sol–gel synthesized sample at 600 °C resulted in change towards a type II N_2-sorption isotherm, which was similar to the one of the reference catalyst. The isotherm for the latter two catalysts showed a flat hysteresis curve in the $0.7 < P/P_0 < 1$ region. Furthermore, the specific surface area for the sol–gel synthesized catalyst was twice as high as the one of the reference catalyst (respectively, 28 and 12 m^2/g). The change in type of sorption isotherms for the sol–gel synthesized samples calcined at 400 and 600 °C, point out that the parallel wands of the slit-shaped pores were slightly distorted by heat treatment.

X-ray analysis of the sol–gel synthesized $Mo_8V_2Sb_{90}O_x$ catalyst, calcined at 400 °C, showed no sharp Bragg reflections, but revealed a long-range superstructure, evident through the broad intense reflections on 1, 0.5 and 0.33 nm (Fig. 1). These reflections immediately can be identified to originate from a layer structure, with an average repetition distance of ≈1 nm. Next to the three strong broad reflections due to the layer structure, the X-ray pattern also shows features reminiscent of Sb_xO_y. This indicates that the materials at least in part are built from antimony oxides. For the catalyst with the same elemental composition, but calcined at 600 °C, the crystalline phases became more pronounced and have been identified as Sb_2O_5 (JCPDS 11-0690), Sb_6O_{13} (JCPDS 33-0111) and Sb_2O_4 (JCPDS 36-1163). The phases

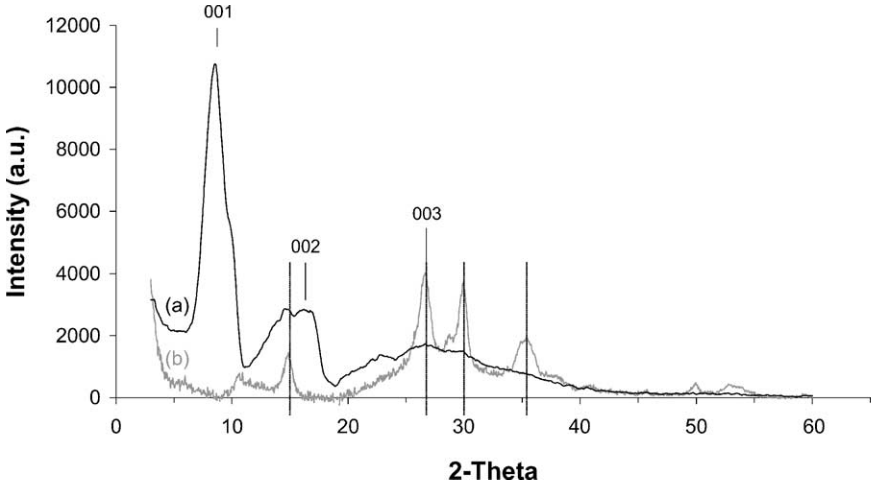

Fig. 1. Transmission XRD pattern of a sol–gel synthesized $Mo_8V_2Sb_{90}O_x$ sample calcined at (a) 400 °C and (b) 600 °C.

arising from the reference catalyst were identified to originate from α-Sb_2O_4 and corresponded to those reported by Shishido et al. [11]. Calcining the slurry synthesized $Mo_8V_2Sb_{90}O_x$ catalyst at 400 °C, resulted in a mainly amorphous material and very little Sb_xO_y crystallinity.

Comparison of the XRD patterns for the reference catalyst and the sol–gel catalysts with the same elemental composition and both calcined at 600 °C, demonstrated the presence of different crystalline structures and the absence of significant amorphous phases in the reference catalyst.

After a catalytic experiment, where the sol–gel synthesized $Mo_8V_2Sb_{90}O_x$ catalyst calcined at 400 °C was tested 24 h at 400 °C and under the mentioned oxygen/isobutane/helium feed, the Sb_xO_y crystalline phases, corresponding to Sb_2O_5, Sb_6O_{13} and Sb_2O_4 mentioned above, became more pronounced.

TEM measurements of the sol–gel synthesized $Mo_8V_2Sb_{90}O_x$ samples, calcined at 400 °C, showed clusters of particles with a size range between 500 and 2000 nm. For these particles mainly a mixture of dominating amorphous and nanocrystalline areas were detected. However, it was difficult to study these crystalline regions because the material is highly sensitive to electron beam damage. For the sol–gel synthesized $Mo_8V_2Sb_{90}O_x$ samples, calcined at 600 °C, particles with a size range between 5 and 10 μm were detected. The latter structures clearly showed distinctive plate-shaped crystalline phases, fused with a bulk phase (Fig. 2). Comparing the results from the X-ray diffraction experiments these crystalline domains could be identified with antimony oxides. The bulk phase had an amorphous character as evident from the absence of sharp reflections in the electron diffraction pattern. Finally, the reference catalyst showed crystals in the 0.5 and 2 μm range. These structures could be identified to fully originate from α-Sb_2O_4.

After calcination at 400 °C in air, the $Mo_8V_2Sb_{90}O_x$ sol–gel synthesized sample exhibited a typical V(IV) EPR spectrum (Fig. 3a). Tetravalent vanadium ($S = 1/2$ and $3d^1$ electron configuration) displays quite a complex EPR spectrum, due to the high number of hyperfine lines arising from the interaction of the unpaired electron with the ^{51}V nucleus (nuclear spin = 7/2) and to the anisotropy of both g and A tensors. The experimental spectrum in Fig. 3a has been reproduced by computer simulation (Fig. 3b) using two V(IV) signals: (i) an axially symmetric signal with $g_{\parallel} = 1.934$, $A_{\parallel} = 206$ G, $g_{\perp} = 1.982$, $A_{\perp} = 70$ G and (ii) an isotropic signal with $g_{iso} = 1.980$ (hyperfine structure not resolved). In line with the assignments of Paganini et al.

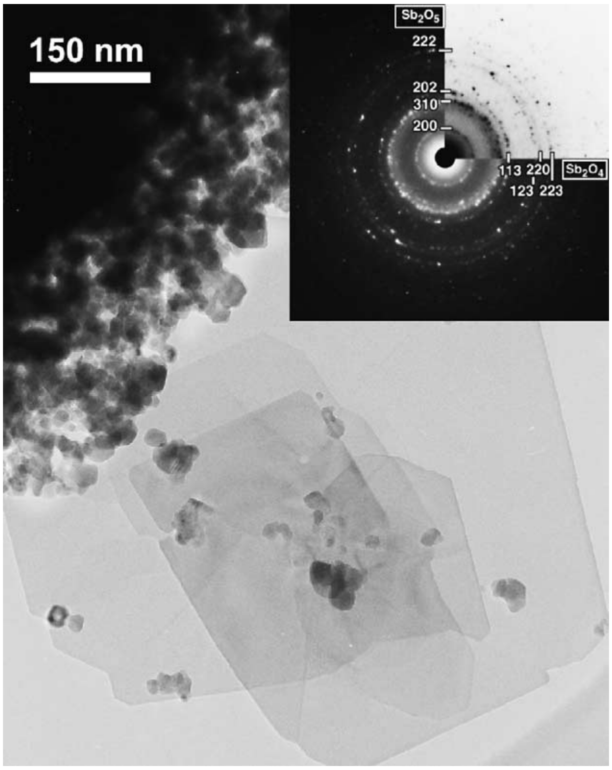

Fig. 2. Representative TEM image of a sol–gel synthesized $Mo_8V_2Sb_{90}O_x$ sample calcined at 600 °C: the insert shows the electron diffraction pattern of the plate-shaped crystalline phase.

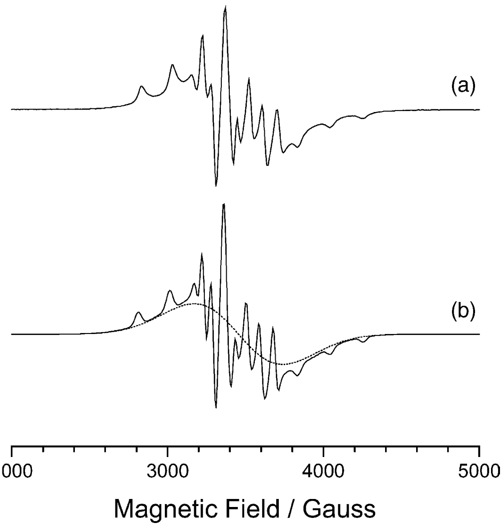

Fig. 3. (a) Experimental EPR spectrum (120 K) of the sol–gel synthesized $Mo_8V_2Sb_{90}O_x$ sample calcined at 400 °C in air, (b) simulated EPR spectrum (full line) with the isotropic contribution in dotted line.

[19], the axial and isotropic signals can be attributed to isolated 5-/6-coordinated vanadyl species and to magnetically interacting V(IV) ions, respectively. The latter study also reported that the occurrence of V(IV) in an oxidized material such as the calcined samples is typical of ternary samples.

For the $Mo_8V_2Sb_{90}O_x$ sol–gel synthesized sample calcined at 600 °C, the hyperfine structure of the EPR spectrum was less pronounced in comparison to the sample calcined at 400 °C. This finding points at a decreasing fraction of isolated V(IV) species upon increasing calcination temperature. In the EPR spectra of both samples after catalytic reaction, the hyperfine structure had almost fully disappeared and only a broad isotropic signal remained. Finally, the EPR spectrum of the fresh slurry synthesized catalyst calcined at 600 °C, did not show any hyperfine structure. This suggests that isolated V(IV) species were absent in this sample.

Quantitative estimation of the amount of paramagnetic species for the sol–gel synthesized $Mo_8V_2Sb_{90}O_x$ sample, calcined at 400 and 600 °C, yields 52 and 45% of V(IV) of the total amount of vanadium, respectively. The latter calculations are based on the assumption that the isotropic signal is fully caused by V(IV) and not by Mo(V).

3.2. Selective isobutane oxidation

Comparison at 400 °C of the sol–gel catalyst calcined at 400 and 600 °C with the slurry phase catalysts with the same composition and calcined at the same temperatures, shows similar conversions (Fig. 4). The slurry phase catalyst with literature composition shows enhanced conversion.

On the other hand, the CO_x selectivity at this conversion, drastically decreases from 46 and 35% for the slurry type catalyst to 33 and 18% for the sol–gel catalysts with the same composition, calcined at 600 and 400 °C, respectively. This decrease in CO_x selectivity is compensated for by an increase in isobutene selectivity. The selectivity to methacrolein remains approximately the same (between 28 and 30%) for both samples calcined at the same temperature. Particularly, for the sol–gel synthesized catalyst calcined at 600 °C, the isobutene and methacrolein selectivity amounts to 24 and 27%, respectively, whereas the values of 19 and 28% are achieved with the slurry phase catalyst of the same composition. When the sol–gel synthesized catalyst is only pre-calcined at 400 °C, the latter values increase up to 30 and 43%, respectively, compared to 30 and 32%, for the slurry phase catalysts. The enhanced activity of the slurry phase literature reference catalyst [11] entirely stems from an enhanced CO_x selectivity.

Time on-stream experiments [12] showed that for the sol–gel synthesized catalysts calcined at 400 and 600 °C the activity increased whereas the selectivity towards the partial oxidation products slightly decreased. This decrease was compensated by an increase in CO_x selectivity.

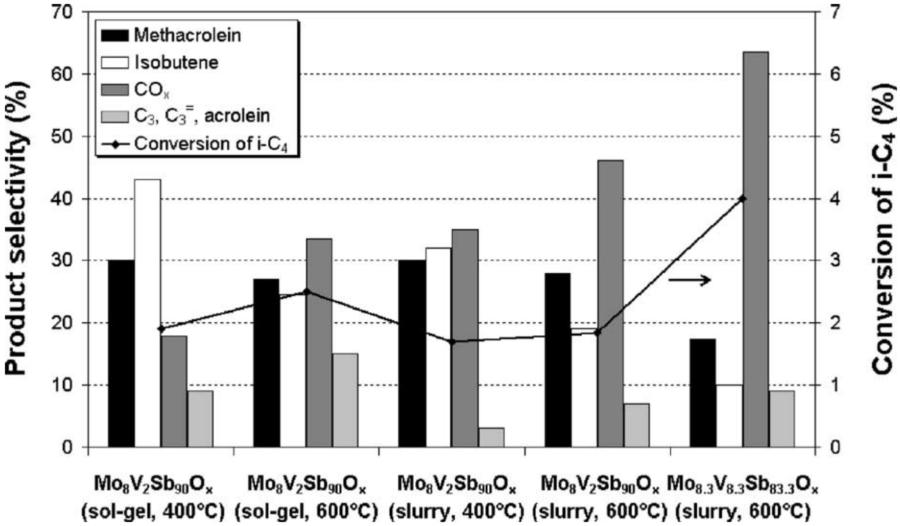

Fig. 4. Product selectivities for the selective oxidation of isobutane at 400 °C for the sol–gel synthesized samples compared to the reference catalyst.

4. Conclusions

The use of a new sol–gel recipe allowed to synthesize homogeneous multi-component oxides with particular physico-chemical properties. Calcination of the samples at 400 °C resulted in a layered superstructure. Additionally, the presence of a large amount of isolated vanadium (IV) sites could be determined, which could not be found in the reference catalyst. The use of enhanced calcination temperatures resulted in the appearance of new crystalline phases in the catalysts and collapse of the layer structure. The enhancement of the catalytic properties for both catalysts compared to the reference catalyst, pointed to the importance of site isolation and unique chemical composition of the samples.

Acknowledgements

This work was performed in the frame of a G.O.A. project supported by the Flemish government. The authors also acknowledge FWO Flanders for grant no. G0231.03 on Combinatorial Catalysis. JP acknowledges KULeuven for a fellowship as Research Assistant. CEAK and MHG acknowledge the FWO Flanders for a research position and a postdoctoral fellowship, respectively. Discussions with Pierre-Alain Weiss and Jens Saalfrank are acknowledged.

References

[1] N. Yoshihiko, O. Motomasa, N. Koichi, S. Hiroshi, Sumitomo Chemical Company, EP 0418657 A2 (1990).
[2] Y. Setsuo, Y. Tatsuo, Asahi Chemical Industries, US Patent 5,191,116 (1993).
[3] K. Yuichi, O. Hideo, Nippon Catalytic Chem. Ind., US Patent 6476259 B2 (2001).
[4] M. Misono, N. Mizuno, K. Inumaru, G. Koyano, X.-H. Lu, Stud. Surf. Sci. Catal. 110 (1997) 118.
[5] K. Inumaru, A. Ono, H. Kubo, M. Misono, J. Chem. Soc. Faraday 94 (1998) 1765.
[6] N. Mizuno, H. Yahiro, J. Phys. Chem. B 102 (1998) 437.
[7] M. Langpape, J.M. Millet, U.S. Ozkan, P. Delichere, J. Catal. 182 (1999) 148.
[8] M. Misono, Topics Catal. 21 (2002) 89.
[9] T. Inoue, K. Asakura, W. Li, S.T. Oyama, Y. Iwasawa, Appl. Catal. A 165 (1997) 183.
[10] T. Inoue, K. Asakura, Y. Iwasawa, J. Catal. 171 (1997) 457.
[11] T. Shishido, T. Inoue, I. Matsuura, K. Takehira, Catal. Lett. 68 (2000) 215.
[12] J.S. Paul, J. Urschey, P.A. Jacobs, W.F. Maier, F. Verpoort, J. Catal. 220 (2003) 136.
[13] J.S. Paul, P.-A.W. Weiss, P.A. Jacobs, W.F. Maier, Appl. Catal. A, in press.
[14] W.F. Maier, I.-C. Tilgner, M. Wiedorn, H.-C. Ko, Adv. Mater. 5 (1993) 726.
[15] Simpow program, Illinois EPR Research Center, Urbana-Champaign, USA.
[16] W.F. Maier, J.A. Martens, S. Klein, J. Heilmann, R. Parton, K. Vercruysse, P.A. Jacobs, Angew. Chem. Int. Ed. 35 (1996) 180.
[17] J.H. de Boer, The shapes of capillaries. In: D.H. Everett, F.S. Stone (Eds.), The Structure and Properties of Porous Materials, Butterworths, London, 1958, p. 68–94.
[18] G. Horvath, K. Kawazoe, J. Chem. Eng. Jpn. 16 (1983) 470.
[19] M.C. Paganini, L. Dall'Acqua, E. Giamello, L. Lietti, P. Forzatti, G. Busca, J. Catal. 166 (1997) 195.